IEEE Access
Multidisciplinary | Rapid Review | Open Access Journal

Received 20 January 2023, accepted 12 February 2023, date of publication 22 February 2023, date of current version 27 February 2023.

Digital Object Identifier 10.1109/ACCESS.2023.3247606

RESEARCH ARTICLE

Modeling and Experimental Evaluation of Haptic Localization Using Electrostatic Vibration Actuators

SANTOSH MOHAN RAJKUMAR[1], KUMAR VIKRAM SINGH[1], TAE-HEON YANG[2], AND JEONG-HOI KOO[1]

[1]Department of Mechanical and Manufacturing Engineering, Miami University, Oxford, OH 45056, USA
[2]Department of Electronic Engineering, Korea National University of Transportation, Chungju-si, Chungcheongbuk-do 27469, Republic of Korea

Corresponding authors: Tae-Heon Yang (thyang@ut.ac.kr) and Jeong-Hoi Koo (koo@miamioh.edu)

This work was supported in part by the Korea National University of Transportation Industry-Academy Cooperation Foundation (2021) and in part by Basic Science Research Program through the National Research Foundation of Korea (NRF) under Grant NRF-2021R1I1A3059609.

ABSTRACT Touch screen devices have become ubiquitous in modern day-to-day lives. While smaller touchscreen devices provide enough user engagement with meaningful haptic feedback, large touch devices still lack meaningful haptic stimulation. Existing literature for large touch surface vibrotactile localization uses many actuators and conventional boundary conditions. Previous numerical studies on haptic localization do not address multi-frequency excitation. This research proposes a new spring-damper boundary condition for a large bar-type display. Subsequently, a mechanical model of the large touch bar surface with multiple-electrostatic vibration actuators is developed using material damping information with multi-frequency excitation. Simultaneously, an experimental setup is developed for validation of the developed model. An optimization technique to localize vibrotactile haptic rendering at multiple selected zones of the touch bar is proposed. It has been established that by varying frequencies of excitation of two electrostatic resonant actuators, localizable vibrotactile feedback can be generated across the length of the touch bar. The experimental results corroborate the simulation results. Finally, the proposed optimization strategy for multi-zone vibrotactile rendering is experimentally verified.

INDEX TERMS Vibration modeling, vibration analysis, localization, localized haptic feedback, electrostatic vibration actuator.

I. INTRODUCTION

Touch screen displays (TSDs) are gaining increasing popularity in modern electronic devices due to their flexibility and the possibility of delivering other modes of interaction than audio and visual modes (e.g., gesture and haptic modes) [1]. TSDs are currently dominating the smartphone and tablet devices industry. Recently, TSDs of tablet devices and personal computers have become larger in size. For example, Apple iPad pro (∼13 inches), Samsung Galaxy Tab S8 ultra (∼14.6 inches), and Microsoft Surface Pro 8 (∼13 inches). Large TSDs (such as 12 inches or more in size) have found utility in automotive infotainment systems/center consoles [2], virtual reality (VR) systems, and immersive gaming [3]. Moreover, large TSDs also find applications in interactive education and training (such as tablet-based learning for children [4], interactive tabletop medical training [5], and digital musical instruments [6]. Large TSDs can also be used in assistive technologies for people with impaired vision and hearing disorders [7]. Presently, large TSDs are being utilized in a multitude of applications, such as information kiosks (at places like restaurants, shopping malls, and airports [8]), and robotic teleoperation interfaces [9].

Contrary to small TSDs found in mobile devices, the major issue with large TSDs is the absence of haptic feedback or the deficiency of meaningful haptic feedback [10]. TSDs with meaningful haptic sensation can enhance user experience by improving the functionality, and the accuracy of inputs [8].

The associate editor coordinating the review of this manuscript and approving it for publication was Lei Wei.

In automotive center consoles, large TSDs without haptic feedback make the driver feel the loss of familiar physical control and can lead to driver distraction [2]. In digital musical instruments using large touch surfaces, haptic feedback is necessary to improve the performance and enable the instrument to be used by performers with hearing or visual impairment [11]. Therefore, there is an increasing requirement for large TSDs to have haptic feedback.

One of the major reasons for the absence of haptic feedback in large TSDs is the availability of a very small number of actuators capable of rendering tactile feedback for large TSDs [12]. Among different actuation strategies for haptic rendering in TSDs, vibrotactile actuation has become the preferred choice because of its affordability, simplified design, and low power consumption [13]. Some of the actuators in use for vibrotactile feedback generation in TSDs include linear resonant actuators (LRAs), eccentric rotary mass (ERM) actuators, piezoelectric actuators, controllable fluid (for e.g., magnetorheological or MR fluid and electrorheological or ER fluid) actuators, and electrostatic actuators [14], [15]. The most important parameters of a feasible actuator for large TSDs are fast response time, almost no residual vibrations, low power consumption, high vibration intensity, and its dimensions. LRA and ERM actuators have slow response times and significant residual vibrations. Controllable fluid actuators are not practical due to their larger size. Piezoelectric actuators are viable for large TSDs due to their fast response and high vibration intensity. The limitations of piezoelectric actuators are high power consumption and their cost. Electrostatic actuators are typically found in parallel plate configurations, and they have fast response, almost no residual vibration, low power consumption, and compact dimensions [14]. They are limited in vibration intensity due to the snap-in phenomenon, which limits the displacement range [16]. Modified dual electrode electrostatic actuators termed electrostatic resonant actuators (ERAs) are found to have sufficient vibration intensity for large TSDs [12], [17].

Another challenge of haptic rendering in large TSDs with a feasible actuator type is to make tactile feedback available throughout the surface of the TSD [14]. Most previous studies effectively tried to generate tactile feedback across the touch surface. However, frequently there exist dead zones or nodes with no haptic feedback on large TSDs [18]. This can be attributed to the use of conventional boundary conditions such as fixed and pinned. For example, a fixed boundary condition requires a drastic change in the actuator's frequency of excitation to change the vibration mode shape of the touch surface [17]. Therefore, there is a need to explore non-conventional (mostly not found in literature) boundary conditions to eliminate dead zones of vibration and to conveniently make haptic feedback available across the whole surface of a large TSD.

With a feasible vibrotactile actuator and suitable boundary conditions, the generation of localized tactile feedback in large TSDs is still challenging due to the need to control waves traveling through them [8]. Localized haptic sensations are required for multi-user tabletop medical training, multi-segment automotive center console, interactive education, multi-touch haptics, VR, and immersive gaming. Different methods are proposed in the literature for generating localized vibrotactile feedback on large touch surfaces. Localized vibration rendering is achieved on large surfaces in the ultrasonic frequency range using Eigen function superposition [19] and time reversal wave focusing [18], [20], [21]. Another approach to localized vibrotactile rendering is the confinement of vibrotactile stimulation above the actuator in narrow plates [22]. The inverse filter method produces localized vibrotactile feedback using a finite number of piezo actuators in the human vibrotactile range [23]. Localized vibrations in the 200-300 Hz range are reported to be achieved using a generalized adversarial network (GAN) to generate time-reversed signals [24]. Superimposition of vibration modes can also lead to localized vibrotactile feedback on large touch surfaces [25], [26]. Except [20], almost all the existing methods of localized vibrotactile rendering require many actuators. The response time of the method presented in [20] is slower for practical applications. Therefore, localized vibrotactile haptic rendering using a small number of actuators on large TSDs still needs further investigation.

Localized vibrotactile haptic stimulation on large TSDs with a limited number of actuators depends on factors like the type of actuators used, the type of excitations, and the placement of the actuators [27]. Physically constructing different large TSD systems with different configurations of these factors is not practical. The development of simulation models for large TSD systems can certainly aid in the exploration of localized vibrotactile feedback on large TSDs with a limited number of actuators. Such mechanical simulation models of large TSDs incorporating vibrotactile actuators also allow us to extend one haptic rendering method to different materials and actuators and find ways of better localization. Finite element modeling of touch surfaces has been discussed with piezo actuators in [28], [29], [30], and [31]. These finite element-based studies focus on generating maximum vibration amplitude on the touch surface rather than localized vibrotactile feedback. Existing finite element-based methods for the simulation of large touch surfaces also lack multi-frequency excitation with multiple actuators, and localized vibrotactile feedback generation is largely unexplored.

As described above, suitable actuators for haptic rendering on large TSDs are not abundant. Using a suitable actuator with conventional rigid boundary conditions make haptic rendering throughout a large TSD challenging. Also, the generation of localized haptic feedback on a large TSD with a limited number of suitable actuators and suitable boundary conditions is largely unexplored. Developing mechanical models of large TSDs with suitable actuators is needed to explore localized haptic rendering. In an effort to generate localized haptic feedback on a large touch surface using a limited number of actuators, this study proposes a narrow

bar-type large touch surface with spring-damper boundary conditions using two electrostatic resonant actuators (ERAs). Such bar-type TSD finds application in automotive center consoles (e.g., climate control systems), home appliances (e.g., microwave oven), laptops (e.g., MacBook Pro's touch bar), etc. In this study, a finite element model of the large touch bar or beam-type display with two ERAs is proposed. The finite element model is based on our previous study [27] with augmentation of material damping and estimated actuator parameters to make it more realistic. The proposed finite element model supports multi-frequency excitations and can be conveniently extended to actuators or touch surfaces of different types. An experimental setup is developed for the large touch bar surface to validate the finite element modeling approach. The physical parameters of the ERAs and the damping of the touch bar are estimated from the practical vibration measurement across the touch bar surface. The possibility of localized vibrotactile feedback generation across the touch bar surface by changing excitation frequencies is shown both experimentally and in simulation. Furthermore, the idea of the localized factor for multi-zone haptics is introduced. An optimization procedure is presented to generate vibrotactile feedback in multiple desired zones of the touch surface.

The organization of the paper is as follows: section II introduces the proposed touch bar with non-conventional boundary conditions followed by finite element modeling and ideas for localized multi-zone vibrotactile feedback, section III describes the experimental setup used in this study, section IV provides results and insights from simulation and experimental study, and section V is the conclusion.

II. MODELING AND SIMULATION

The large TSD considered in this study is a narrow or bar-type display where the ERAs are directly connected, as shown in Figure 1(a). The touch bar is not rigidly fixed on any ends, and the ERAs are capable of exciting it in multiple frequencies. The excitations considered in this study are sinusoidal displacements transmitted from the ERAs to the touch bar through their connections. The excitations of the ERAs can be independently controlled.

A. FINITE ELEMENT MODELING FOR MULTI-FREQUENCY EXCITATION

The direct connection between the actuator(s) and the touch display gives rise to spring-damper boundary conditions as opposed to conventional rigid boundary conditions, as shown in Figure 1(b). The connection between each ERA and the touch bar is made with bolts. Let the displacement amplitude of an ERA be α_i, mass of each bolt be m_{bi}, the stiffness of each ERA be the stiffness is k_{bi}, and the damping coefficient be c_{bi}, for i^{th} ERA. Considering the material to be linear homogeneous, the touch bar can be modeled as Euler-Bernoulli slender beam. The dimensions of the touch bar are defined as length L, width B, and thickness h. Let E be the modulus of elasticity of the beam, ρ be the density of the

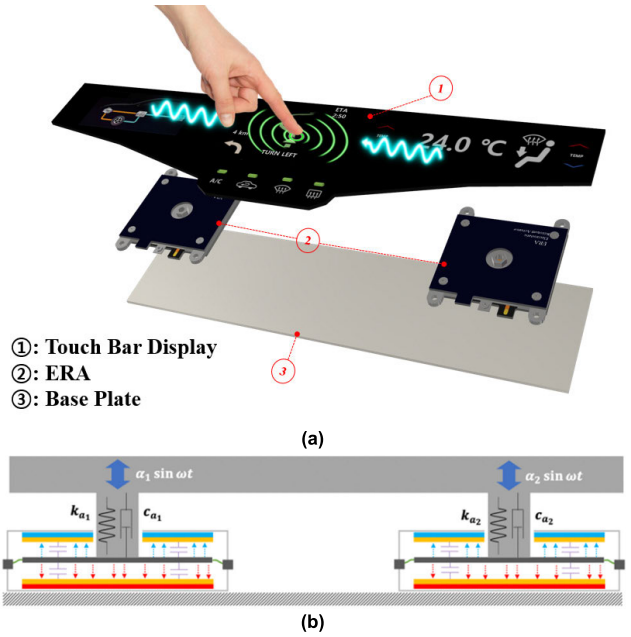

FIGURE 1. Touch-bar display with two ERAs (electrostatic resonant actuators): (a) conceptual illustration of the system, (b) Modeling of the system.

beam, c be the uniform damping of the beam material, I be the uniform second moment of inertia, A be the cross-sectional area, $u(x, t)$ be the transverse displacement, x be the spatial location, and t be the instant of time. The governing equation for forced vibration of a beam under excitation $f(x, t)$ is given as,

$$EI\frac{\partial^4 u(x,t)}{\partial^4 x} + \rho A\frac{\partial^2 u(x,t)}{\partial^2 t} + c\frac{\partial u(x,t)}{\partial t} = f(x,t) \quad (1)$$

We discretize the touch bar into n finite elements ignoring the material damping of the touch bar. Each element consists of two nodes with two degrees of freedom (transverse displacement and slope). We consider that the transverse displacement varies as a cubic polynomial across the length of an element. Using a suitable weight function and variational form of the equation(1), we obtain the elemental mass, stiffness, damping, and external forces matrices as $\mathbf{M}^{\text{e}}$, $\mathbf{K}^{\text{e}}$, $\mathbf{C}^{\text{e}}$, and $\mathbf{f}^{\text{e}}$ respectively. Here, the matrix $\mathbf{C}^{\text{e}}$ contains only the damping due to the ERAs at the boundaries. Assembling the elemental mass, stiffness, damping, and external forces matrices, we obtain their global versions as $\mathbf{M}$, $\mathbf{K}$, $\mathbf{C}_A$, and $\mathbf{f}$. The details on the derivation can be found in [27]. It is important to note that the matrix $\mathbf{C}_A$ contains the damping information at the boundaries due to the actuators only. We consider that the material damping of the touch bar is proportional to mass and stiffness, and given as,

$$\mathbf{C}_M = \sigma\mathbf{M} + \eta\mathbf{K} \quad (2)$$

Therefore, the total damping matrix for the simulation of the dynamics of the touch bar is the material damping matrix with the damping due to the actuators added at the respective

degree of freedoms of boundaries, and it can be expressed as,

$$\mathbf{C} = \mathbf{C}_A + \mathbf{C}_M \tag{3}$$

With $\mathbf{y}$ being the vector containing displacements and slopes of the global nodes, the finite element dynamics of the touch bar can be given as,

$$\mathbf{M}\ddot{\mathbf{y}}(t) + \mathbf{C}\dot{\mathbf{y}}(t) + \mathbf{K}\mathbf{y}(t) = \mathbf{f}(t) \tag{4}$$

For multiple harmonic excitations, the equation (4) can be rewritten as,

$$\mathbf{M}\ddot{\mathbf{y}}(t) + \mathbf{C}\dot{\mathbf{y}}(t) + \mathbf{K}\mathbf{y}(t) = \sum_{i=1}^{m} (\mathbf{s}_i \sin \omega_i t + \mathbf{k}_i \cos \omega_i t) \tag{5}$$

Here, $\mathbf{s}_i$ and $\mathbf{k}_i$ are vectors containing amplitudes of harmonic excitations at i-th degree of freedom. To obtain simulated vibrotactile response at different spatial locations of the touch bar, we have to obtain the solution to the multiple degrees of freedom system of differential equation represented in (5). We use an efficient analytical solution method for that purpose which gives the displacements and slopes across different degrees of freedom of the FE model for zero initial conditions, as shown in equation (6). Details on the derivation of the analytical solution method can be found in [27].

$$\mathbf{y}\,(t) = \sum_{i=1}^{m} (\mathbf{P}_i \cos \omega_i t + \mathbf{Q}_i \sin \omega_i t) \tag{6}$$

Here, $\mathbf{P}_i, \mathbf{Q}_i$ are constant vectors defining harmonic motion with the same frequency ω_i having different amplitudes at different degrees of freedom. The steady-state accelerations at different global nodes of the touch bar are given as [27],

$$\Phi\,(t) = -\sum_{i=1}^{m} \omega_i^2 \,(\mathbf{P}_i \cos \omega_i t + \mathbf{Q}_i \sin \omega_i t) \tag{7}$$

The absolute peak steady-state acceleration at any degree of freedom j of the touch bar is obtained as [27],

$$\Phi_j == \sum_{i=1}^{m} \omega_i^2 \sqrt{(P_j)_i^2 + (Q_j)_i^2} \tag{8}$$

For this study, we have considered the touch bar to be made of Aluminium with E = 70 GPa and $\rho = 2700$ kg / m^3. This finite element modeling strategy can be extended to many actuators with multiple frequencies of excitations. Equation (8) gives the peak steady-state acceleration at the selected finite number of nodes across the touch bar. These nodal accelerations can be interpolated using the shape function to provide peak steady-state acceleration at any point of the touch bar. The vibrotactile feedback intensity at any point is characterized by the magnitude of peak acceleration due to excitations from the ERAs.

FIGURE 2. Showing a selected spatial domain and the total domain.

B. MULTI-ZONE VIBROTACTILE LOCAIZATION

For multi-zone localized vibrotactile feedback, the aim is to segment the touch bar into localized zones where the vibration intensity is much greater than the intensity of vibrotactile feedback on the zones outside of them (non-localized zone). The localized zones are the desired portions of the touch bar where the user wants to have significant vibrotactile feedback and the non-localized zones are portions where vibrotactile feedback is desired to be insignificant. For this study, greater vibration intensity implies greater peak transverse acceleration.

The localized factor for any selected zone of the touch bar can be defined as the ratio of the total kinetic energy of the selected zone to the total kinetic energy of the entire surface [32]. Let us consider Γ_L to be the spatial domain of a selected zone and Γ_T be the spatial domain of the entire touch bar. The kinetic energies at any instant of time for the two domains can be given as [32],

$$\begin{aligned} E(t)|_{\Gamma_L} &= \frac{1}{2}\rho h \int_{\Gamma_L} \left(\frac{\partial u}{\partial t}\right)^2 dA \\ E(t)|_{\Gamma_T} &= \frac{1}{2}\rho h \int_{\Gamma_T} \left(\frac{\partial u}{\partial t}\right)^2 dA \end{aligned} \tag{9}$$

Mathematically, localized factor Λ for a particular zone can be expressed as [32],

$$\Lambda = \frac{\int_{t_0}^{t} E(t)|_{\Gamma_L}\, dt}{\int_{t_0}^{t} E(t)|_{\Gamma_T}\, dt} = \frac{\int_{t_0}^{t}\int_{\Gamma_L} \left(\frac{\partial u}{\partial t}\right)^2 dA dt}{\int_{t_0}^{t}\int_{\Gamma_T} \left(\frac{\partial u}{\partial t}\right)^2 dA dt} \tag{10}$$

The value of Λ can vary from 0 to 1. $\Lambda = 1$ for a particular zone implies vibrotactile response is fully localized at that zone, and $\Lambda = 0$ implies otherwise.

As an example, demonstrating the localized factor concept, we divide the touch bar into five zones. Then the peak steady-state accelerations using the finite element model for 60 Hz & 90 Hz excitations of the ERAs are computed ignoring material damping and using the following parameters,

$$\begin{aligned} k_{a1} &= k_{a2} = 20 \text{ kN/m}, \quad c_{a1} = c_{a2} = 0.0265 \text{ Ns/m} \\ \alpha_1 &= \alpha_2 = 0.42\ \mu\text{m} \end{aligned}$$

The computed localized factor for each zone and the corresponding peak steady state accelerations are shown in figure 3. We observe that at a particular segment of the display, the highest magnitude of peak acceleration is directly proportional to the computed localized factor. For example, section III has the lowest peak acceleration and subsequently the lowest localized factor. Further, section V has the highest

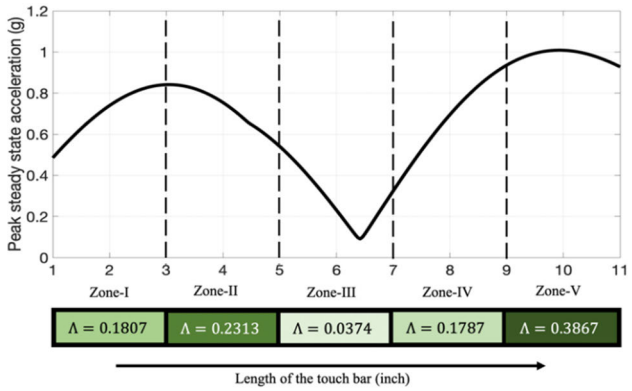

FIGURE 3. Computed localized factor at different zones of the touch bar for dual ERA excitation (60 Hz & 90 Hz).

localized factor and the highest peak acceleration. This simulation result validates the idea of localized factor.

For two actuator excitations of the touch bar system, we can adjust the frequencies of excitation and the displacement amplitudes of the ERAs. Let f_1, f_2 be the set of frequencies of excitation. Therefore, for multi-zone vibration localization, we can maximize localized factors of the desired zones to yield the respective excitation frequencies. The maximization problem for m-localized zones becomes,

$$\arg\max_{f_1,f_2,\alpha_1,\alpha_2} \sum_{i=1}^{m} \Lambda_i \tag{11}$$

Here, Λ_i is the localized factor of i-th desired zone for vibration localization. It is important to note that the total sum of the localized factors of the different zones of the touch bar is unity. Therefore, for multiple selected localized zones after the optimization, the sum of the localized factor of the selected zones will be much larger than the sum of localized factors of the zones not selected. This implies that the selected localized zones will have greater vibration intensity or peak transverse acceleration than the zones not selected.

III. EXPERIMENT DESIGN

A. EXPERIMENTAL SETUP

The ERA comprises two fixed electrodes at the top and bottom, and a moveable mass suspended between the two electrodes. The mass is connected to the electrical ground and suspended using radial beam springs. When an electrode is excited with high voltage, a capacitance is created between it and the grounded mass, and the mass gets attracted to the electrode. The radial beam springs tend to oppose the electrostatic force and try to pull mass back to equilibrium. Thus, the change in forces makes the mass oscillate, providing vibrations needed for actuation. The grounded mass is available for external connection via a hole through the upper electrode and is bolted to the touch bar. The stiffness of the radial beam spring holding the grounded mass describes the actuator stiffness and damping. The two electrodes are excited asynchronously (with a phase gap) to avoid interference. A schematic diagram of a dual-electrode ERA is shown in figure 4.

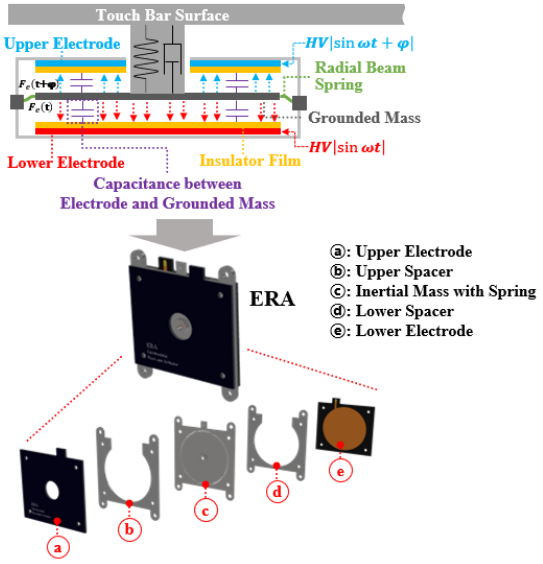

FIGURE 4. Schematic of an electrostatic resonant actuator (ERA).

The experimental setup used for this study consists of a touch bar made of aluminum (E = 70 GPa, $\rho = 2700$ kg/m^3), two ERAs, one tablet-PC for control interface, microprocessor-based voltage control circuitry with two high-voltage amplifiers, one accelerometer, and a data acquisition system. The interface on the tablet PC provides controls for frequencies of excitation, amplitudes, and phase delays of the actuators. The tablet-PC communicates with the microprocessor of the control circuit via Bluetooth, and based on the command received, the control circuit provides actuation signals to the ERAs. The accelerometer used is from PCB Piezotronics Inc. with high sensitivity of 1.02 mV/(m/s^2), a frequency range of 0.5-10 kHz, lightweight (2 gm), and a measurement range of up to $\pm$50 g acceleration. The data acquisition system consists of a National Instruments c-DAQ board and is interfaced with MATLAB. The ERAs are bolted to the touch bar at positions 0.16 L (left side) and 0.977 L (right side).

B. ESTIMATION OF ACTUATOR PARAMETERS AND MATERIAL DAMPING

The actuator parameters like stiffness, the amplitude of displacement, and the material damping co-efficients (σ, η) need to be estimated from practical data for making the mechanical model of the touch bar more realistic. It is also important to note that the actuators are bolted to the touch bar, which might affect the stiffness of each actuator. We consider that the actuator damping and maximum displacement amplitude are the same for both actuators (i.e. $c_{a1} = c_{a2} = c_a$, and $\alpha_1 = \alpha_2 = \alpha$). To estimate these parameters, we excite the touch bar with a range of frequencies using both the ERAs with 100% of the displacement amplitudes and collect the peak acceleration amplitudes at 22 points across the length of the touch bar. We initialize the actuator parameters and material damping to arbitrary values based on heuristics and

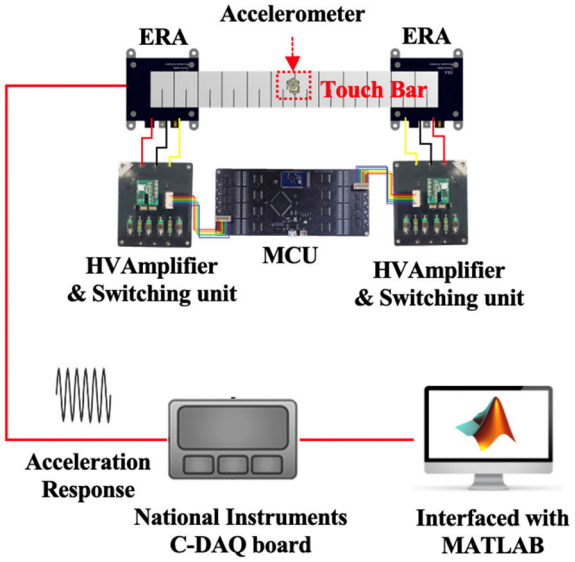

FIGURE 5. The experimental set up.

simulate the touch bar model with dual actuators at the same 22 points where we collected experimental data. The optimization objective function to estimate k_{b1}, k_{b2}, α, c_a, σ, and η become,

$$\underset{k_{a1},k_{a2},\alpha,c_a,\sigma,\eta}{\arg\min} \quad J(k_{a1}, k_{a2}, \alpha, c_a, \sigma, \eta) = \sum_{k=1}^{22} \left| \Phi_k - \tilde{\Phi}_k \right| \quad (12)$$

Here, Φ_k is the peak acceleration measured at point k and $\tilde{\Phi}_k$ is the simulated peak acceleration at point k. To solve the optimization problem in equation (12), we used MATLAB's constrained optimization solver *fmincon*. This solver is gradient-based and uses the sequential quadratic programming (SQP) method. The constraints for the parameters to be estimated using the optimization are provided based on heuristics and domain knowledge provided in [8] and [27]. For each frequency pair, we estimated the parameters using optimization and took the average to obtain the final parameter values. The estimated parameters and damping coefficient are found to be as follows,

$$k_{a1} = 18.9 \text{ kN/m}, \quad k_{a2} = 17.5 \text{ kN/m}, \quad c_a = 0.045 \text{ Ns/m}$$
$$\alpha = 0.52\ \mu\text{m}, \quad \sigma = 1.008e^{-5}, \eta = 5.00456e^{-5}$$

IV. RESULTS

Using the estimated parameters of the two ERAs and the damping of the touch bar material, the finite element model of the touch bar is simulated, and the vibrotactile response across the length of the touch bar is computed. Practical vibrotactile responses at 22 locations across the length of the touch bar are obtained for comparison. The locations with insignificant vibration will be referred to as nodes. Neutralizing a node is to make the vibration of the node a significant one. We consider two scenarios: 1) when the touch bar is excited with a single actuator and 2) when the touch bar is excited with both actuators. In both scenarios, the actuators are activated with 100% displacement amplitude.

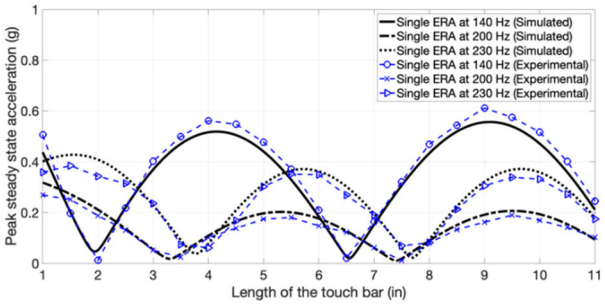

FIGURE 6. Comparison between computed vibrotactile response and experimentally measured vibrotactile response across the length of the touch bar when a single actuator is activated.

For a single actuator scenario, three excitation frequencies (140 Hz, 200 Hz, and 230 Hz) are used. Figure 6 shows the comparison of experimental vibration response and simulated vibration response across the length of the touch bar for single actuator excitation. A clear variable vibrotactile response pattern is observed with the change in excitation frequencies. For example, when excited with 140 Hz frequency, there is a node around 2 inches in length, which can be neutralized by switching to 230 Hz frequency or 200 Hz frequency. The node around 4 inches in length of the touch bar during 230 Hz excitation can be neutralized by switching the frequency to 140 Hz. The experimental vibration response obtained is like the simulated response. However, the vibration intensity obtained using a single actuator is insignificant and may not be sufficient to provide a meaningful haptic experience to the user.

For a dual actuator scenario, three sets of frequencies are considered (150 Hz and 130 Hz, 150 Hz, and 200 Hz, and 150 Hz and 230 Hz). Compared to a single actuator case, the vibrotactile responses obtained with two actuators are significantly greater. Figure 7 compares experimental and simulated vibration response across the length of the touch bar for dual actuator excitation. Figure 7 shows that the node point nearly 2 inches in length during 150 Hz and 200 Hz excitation can be neutralized by switching to 150 Hz and 130 Hz or 150 Hz and 230 Hz excitation. Also, the vibrotactile intensity between the point near 6 inches in length during 150 Hz and 130 Hz excitation can be intensified by switching to 150 Hz and 230 Hz excitation. The experimental vibrotactile response obtained for dual actuators corroborates the simulated vibrotactile response. We have observed experimentally and in simulation that vibrotactile response across the length of the touch bar can be localized by switching between various excitation frequencies. A peak acceleration greater than 1.5 g can be achieved throughout the touch bar without any dead zones.

For a demonstration of multi-zone vibration localization, we perform the optimization operation given in equation (11) to localize vibrotactile feedback in zones I, III, and V. The optimization operation is performed in simulation with the finite element model of the touch bar using MATLAB's constrained optimization solver *fmincon*. Since MATLAB's

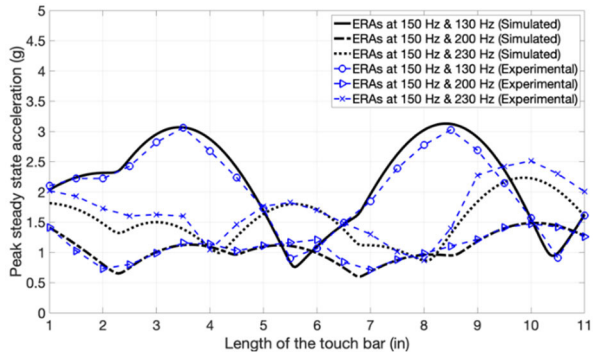

FIGURE 7. Comparison between computed vibrotactile response and experimentally measured vibrotactile response across the length of the touch bar when both the two actuators are activated.

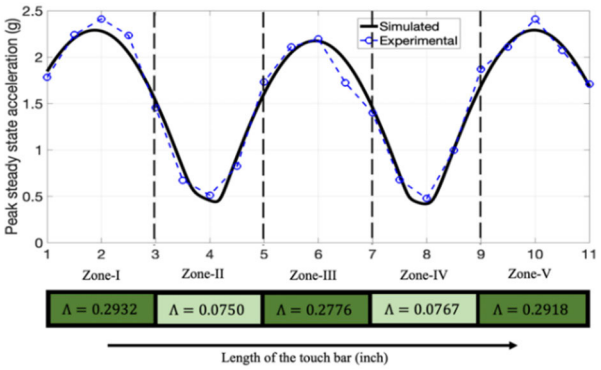

FIGURE 8. Multi-zone vibrotactile feedback localization using optimization at zones I, III, and V.

fmincon minimizes the objective function, we used the negative of the objective function to get it maximized. The excitation frequencies and displacements of the ERAs obtained from the optimization process are used to excite the touch bar and the vibrotactile response obtained across the touch bar is shown in figure 8 with the value of the maximized objective function as 0.8626. We observe that the localized factors at zones I, III, and V are significantly higher than those at zones II and IV. Similarly, the magnitudes of peak accelerations at zones I, III, and V are significantly higher than those at zones II and IV. The agreement of the peak acceleration graph obtained in the simulation to the experimental study with the optimized excitation parameters also corroborates the efficacy of the proposed method. Therefore, the proposed optimization approach can be used to obtain localized vibrotactile feedback at multiple desired zones of the touch bar.

V. CONCLUSION

In this study, we introduced a non-conventional boundary condition for a large touch bar type display where electrostatic actuators (ERAs) are directly attached to it. A finite element-based mechanical model formation of the touch surface with multiple ERAs using material damping information is discussed. An experimental setup is developed using an aluminum touch bar with two ERAs. The physical parameters and the material damping information are estimated for the mechanical model from experimental data using an optimization strategy. The idea of localized factor has been introduced, and it has been shown that localized factor directly relates to vibrotactile output at a particular zone. An optimization technique to generate localized vibrotactile feedback at multiple desired zones of the touch bar is proposed. It has been shown that various localizable vibrotactile feedback can be generated across the length of the touch bar by varying excitation frequencies of the two ERAs. Both experimental and simulation studies affirmed the localized vibrotactile feedback generation strategy with excitation frequency variations. Finally, it is demonstrated that optimizing the localized factors of multiple desired zones towards their maximum leads to the maximum vibration intensity at the desired zones. This modeling and rendering technique presents a methodology that can effectively provide multi-point vibrotactile feedback in response to the rapidly spreading large-screen multi-touch technology.

Future research directions of this study can explore real-time multi-zone haptic localization strategy. Also, studying the resolution of localized haptic rendering with a limited number of actuators can be a future research direction.

ACKNOWLEDGMENT

(Tae-Heon Yang and Jeong-Hoi Koo contributed equally to this work.)

REFERENCES

[1] E. Hoggan, S. A. Brewster, and J. Johnston, "Investigating the effectiveness of tactile feedback for mobile touchscreens," in *Proc. SIGCHI Conf. Hum. Factors Comput. Syst.*, Apr. 2008, pp. 1573–1582.
[2] K. Klein, "Rethinking touch HMI controls for automotive displays and smart surfaces," *Inf. Display*, vol. 38, no. 1, pp. 24–29, Jan. 2022.
[3] D. Wang, Y. Guo, S. Liu, Y. Zhang, W. Xu, and J. Xiao, "Haptic display for virtual reality: Progress and challenges," *Virtual Reality Intell. Hardw.*, vol. 1, no. 2, pp. 136–162, Apr. 2019, doi: 10.3724/SP.J.2096-5796.2019.0008.
[4] D. Cingel and A. M. Piper, "How parents engage children in tablet-based reading experiences: An exploration of haptic feedback," in *Proc. ACM Conf. Comput. Supported Cooperat. Work Social Comput.*, Feb. 2017, pp. 505–510, doi: 10.1145/2998181.2998240.
[5] U. von Zadow, S. Buron, T. Harms, F. Behringer, K. Sostmann, and R. Dachselt, "SimMed: Combining simulation and interactive tabletops for medical education," in *Proc. SIGCHI Conf. Hum. Factors Comput. Syst.*, 2013, pp. 1469–1478.
[6] C. H. Mejia, P. Germano, S. C. Echeverri, and Y. Perriard, "Artificial neural networks for impact position detection in haptic surfaces," in *Proc. IEEE Int. Ultrason. Symp. (IUS)*, Oct. 2019, pp. 1874–1877.
[7] F. Sorgini, R. Caliò, M. C. Carrozza, and C. M. Oddo, "Haptic-assistive technologies for audition and vision sensory disabilities," *Disab. Rehabil., Assistive Technol.*, vol. 13, no. 4, pp. 394–421, May 2018, doi: 10.1080/17483107.2017.1385100.
[8] T. W. Mason, "Design and testing of an electrostatic actuator with dual-electrodes for large touch display applications," M.S. thesis, Dept. Mech. Manuf. Eng., Miami Univ., Oxford, OH, USA, 2021.
[9] R. Luz, J. Corujeira, L. Grisoni, F. Giraud, J. L. Silva, and R. Ventura, "On the use of haptic tablets for UGV teleoperation in unstructured environments: System design and evaluation," *IEEE Access*, vol. 7, pp. 95443–95454, 2019, doi: 10.1109/access.2019.2928981.
[10] S. Park, D. Kim, W. Kim, and N.-C. Park, "Rendering high-fidelity vibrotactile feedback on a plate via optimization of actuator driving signals," in *Proc. Inter-Noise Noise-Con Congr. Conf.*, vol. 261, no. 6, 2020, pp. 548–555.

[11] C. Hernandez-Mejia, M. Favier, X. Ren, P. Germano, and Y. Perriard, "Reinforcement learning and hardware in the loop for localized vibrotactile feedback in haptic surfaces," in *Proc. IEEE Int. Ultrason. Symp. (IUS)*, Sep. 2021, doi: 10.1109/IUS52206.2021.9593749.

[12] T. Mason, J.-H. Koo, Y.-M. Kim, and T.-H. Yang, "Experimental evaluation on the effect of electrode configuration in electrostatic actuators for increasing vibrotactile feedback intensity," *Appl. Sci.*, vol. 10, no. 15, p. 5375, Aug. 2020, doi: 10.3390/APP10155375.

[13] S. Park, W. Kim, D. Kim, J. Kwon, H. Bae, and N.-C. Park, "Vibrotactile rendering on a touch surface with reduced sound radiation," *J. Sound Vibrat.*, vol. 497, Apr. 2021, Art. no. 115936, doi: 10.1016/j.jsv.2021.115936.

[14] C. Basdogan, F. Giraud, V. Levesque, and S. Choi, "A review of surface haptics: Enabling tactile effects on touch surfaces," *IEEE Trans. Haptics*, vol. 13, no. 3, pp. 450–470, Jul. 2020, doi: 10.1109/TOH.2020.2990712.

[15] Y. Jansen, T. Karrer, and J. Borchers, "MudPad: Tactile feedback and haptic texture overlay for touch surfaces," in *Proc. ACM Int. Conf. Interact. Tabletops Surf.*, Nov. 2010, pp. 1–3.

[16] R. W. Johnstone and M. Parameswaran, *An Introduction to Surface-Micromachining*. New York, NY, USA: Springer, 2004, doi: 10.1007/978-1-4020-8021-0.

[17] T. Mason, J.-H. Koo, J.-I. Kim, Y.-M. Kim, and T.-H. Yang, "A feasibility study of a vibrotactile system based on electrostatic actuators for touch bar interfaces: Experimental evaluations," *Appl. Sci.*, vol. 11, no. 15, p. 7084, Jul. 2021, doi: 10.3390/app11157084.

[18] C. Hudin, J. Lozada, and V. Hayward, "Localized tactile feedback on a transparent surface through time-reversal wave focusing," *IEEE Trans. Haptics*, vol. 8, no. 2, pp. 188–198, Apr. 2015, doi: 10.1109/TOH.2015.2411267.

[19] J.-H. Woo and J.-G. Ih, "Vibration rendering on a thin plate with actuator array at the periphery," *J. Sound Vibrat.*, vol. 349, pp. 150–162, Aug. 2015, doi: 10.1016/j.jsv.2015.03.031.

[20] M. R. Bai and Y. K. Tsai, "Impact localization combined with haptic feedback for touch panel applications based on the time-reversal approach," *J. Acoust. Soc. Amer.*, vol. 129, no. 3, pp. 1297–1305, Mar. 2011, doi: 10.1121/1.3533725.

[21] S. Wockel, U. Steinmann, and H. Arndt, "Haptics by time reversal of elastic waves," in *Proc. IEEE Int. Ultrason. Symp. (IUS)*, Sep. 2016, vol. 129, no. 3, pp. 1–3, doi: 10.1109/ULTSYM.2016.7728754.

[22] A. B. Dhiab and C. Hudin, "Confinement of vibrotactile stimuli in narrow plates: Principle and effect of finger loading," *IEEE Trans. Haptics*, vol. 13, no. 3, pp. 471–482, Jul. 2020, doi: 10.1109/TOH.2020.2986727.

[23] L. Pantera and C. Hudin, "Multitouch vibrotactile feedback on a tactile screen by the inverse filter technique: Vibration amplitude and spatial resolution," *IEEE Trans. Haptics*, vol. 13, no. 3, pp. 493–503, Jul. 2020, doi: 10.1109/TOH.2020.2981307.

[24] C. Hernandez-Mejia, X. Ren, A. Thabuis, J. Chavanne, P. Germano, and Y. Perriard, "Generative adversarial networks for localized vibrotactile feedback in haptic surfaces," in *Proc. 24th Int. Conf. Electr. Mach. Syst. (ICEMS)*, 2021, pp. 105–110, doi: 10.23919/ICEMS52562.2021.9634513.

[25] K. Katumu and J. L. Gorlewicz, "Using modal superposition for generating localized tactile effects on variable friction touchscreens," in *Proc. IEEE Haptics Symp. (HAPTICS)*, Apr. 2016, pp. 211–216, doi: 10.1109/HAPTICS.2016.7463179.

[26] E. Enferad, C. Giraud-Audine, F. Giraud, M. Amberg, and B. L. Semail, "Generating controlled localized stimulations on haptic displays by modal superimposition," *J. Sound Vibrat.*, vol. 449, pp. 196–213, Jun. 2019, doi: 10.1016/j.jsv.2019.02.039.

[27] S. M. Rajkumar, K. V. Singh, and J.-H. Koo, "Modeling and analysis of multiple electrostatic actuators on the response of vibrotactile haptic device," in *Proc. ASME Int. Mech. Eng. Congr. Expo.* New York, NY, USA: American Society of Mechanical Engineers, vol. 86625, 2022, p. 10.

[28] B. Baylan, U. Arindogan, and C. Basdogan, "Finite Element Modeling of a Vibrating Touch Screen Actuated by Piezo Patches for Haptic Feedback," in *Proc. Int. Conf. Human Haptic Sens. Touch Enabled Comput. Appl.*, 2012, pp. 47–57.

[29] N. L. Alpdoğan and M. Ayyildiz, "Towards localized tactile feedback on touch surfaces: Finite element analysis of a vibrating touch screen actuated by piezo patches," *Eur. J. Sci. Technol.*, vol. 2021, no. 29, pp. 214–218, Dec. 2021, doi: 10.31590/ejosat.1014803.

[30] A. F. Ak, G. Sari, M. B. Akgul, B. Kirisken, and A. A. Akis, "Numerical analysis of vibrating touch screen actuated by piezo elements," in *Proc. 8th Int. Conf. Mech. Aerosp. Eng. (ICMAE)*, Jul. 2017, pp. 775–779.

[31] R. Le Magueresse, F. Casset, F. Giraud, B. Desloges, N. David, A. Kaci, A. Berdague, and M. Colin, "Piezoelectric flexible haptic interface development," in *Proc. 23rd Int. Conf. Thermal, Mech. Multi-Physics Simul. Experiments Microelectron. Microsystems (EuroSimE)*, Apr. 2022, pp. 1–5, doi: 10.1109/EuroSimE54907.2022.9758912.

[32] J. Park, "Method for generating multi-point vibrotactile feedback based on electrostatic panel actuator," M.E. theses, Master School Mech. Aerosp. Eng., Korea Adv. Inst. Sci. Technol. (KAIST), Daejeon, South Korea, 2021.

SANTOSH MOHAN RAJKUMAR received the bachelor's degree in electrical engineering from the National Institute of Technology at Silchar, Silchar, India, in 2017. He is currently pursuing the master's degree in mechanical engineering with Miami University, Oxford, OH, USA. In 2017, he joined Indian Oil Corporation Ltd. (a Fortune 200 Company) as a Senior Engineer, where he worked until he began his M.S. Program. His research interests include dynamical systems, control, and robotics, with a particular focus on their application in the fields of human–computer interaction, haptics, assistive and rehabilitation devices, and data-driven modeling and control methods.

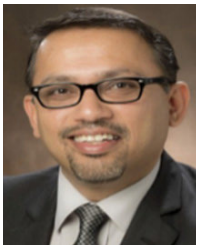

KUMAR VIKRAM SINGH received the B.E. degree in mechanical engineering from the Birla Institute of Technology at Mesra, Mesra, India, in 1997, and the Ph.D. degree in mechanical engineering from Louisiana State University (LSU), in 2003. In 2006, he joined Miami University after serving as a Postdoctoral Research Associate at LSU. He is currently a Professor with the Department of Mechanical and Manufacturing Engineering. His research interests include theoretical, computational, and applied inverse eigenvalue problems related to multidisciplinary areas of vibration and control. He is an Associate Fellow of the American Institute of Aeronautics and Astronautics (AIAA).

TAE-HEON YANG received the B.S. degree from Yonsei University, Republic of Korea, in 2006, and the M.S. and Ph.D. degrees from the Department of Mechanical Engineering, Korea Advanced Institute of Science and Technology (KAIST), in 2008 and 2012, respectively. From 2012 to 2017, he was a Senior Research Scientist at the Korea Research Institute of Standards and Science. He has been with the Faculty of Electronic Engineering, Korea National University of Transportation, since 2018. His research interests include haptic sensor and actuator, medical simulator, and human–computer interface.

JEONG-HOI KOO received the Ph.D. degree in mechanical engineering from Virginia Tech, in 2003. He is currently a Professor of mechanical and manufacturing engineering with Miami University, Oxford, OH, USA. His research interests include smart materials and systems and humanitarian engineering. He was elected as a fellow of the American Society of Mechanical Engineers (ASME), in 2019. He is also serving as an Associate Editor for the *Journal of Vibration and Control*, *Shock and Vibration Journal*, and *Frontiers in Materials–Smart Materials*.